Natural images dominate in binocular rivalry

Daniel H. Baker[1] and Erich W. Graf

School of Psychology, University of Southampton, Southampton SO17 1BJ, United Kingdom

Edited by Dale Purves, Duke University Medical Center, Durham, NC, and approved February 10, 2009 (received for review December 18, 2008)

Ecological approaches to perception have demonstrated that information encoding by the visual system is informed by the natural environment, both in terms of simple image attributes like luminance and contrast, and more complex relationships corresponding to Gestalt principles of perceptual organization. Here, we ask if this optimization biases perception of visual inputs that are perceptually bistable. Using the binocular rivalry paradigm, we designed stimuli that varied in either their spatiotemporal amplitude spectra or their phase spectra. We found that noise stimuli with ''natural'' amplitude spectra (i.e., amplitude content proportional to 1/*f*, where *f* is spatial or temporal frequency) dominate over those with any other systematic spectral slope, along both spatial and temporal dimensions. This could not be explained by perceived contrast measurements, and occurred even though all stimuli had equal energy. Calculating the effective contrast following attenuation by a model contrast sensitivity function suggested that the strong contrast dependency of rivalry provides the mechanism by which binocular vision is optimized for viewing natural images. We also compared rivalry between natural and phase-scrambled images and found a strong preference for natural phase spectra that could not be accounted for by observer biases in a control task. We propose that this phase specificity relates to contour information, and arises either from the activity of V1 complex cells, or from later visual areas, consistent with recent neuroimaging and single-cell work. Our findings demonstrate that human vision integrates information across space, time, and phase to select the input most likely to hold behavioral relevance.

amplitude spectrum | interocular suppression | natural image statistics | phase spectrum | bistable perception

The human visual system is tasked with processing and organizing perceptual information relevant to the tasks we routinely perform. Recent investigations of the statistical properties of natural images indicate that the tuning characteristics of early visual mechanisms reflect measurable properties of the world (1). From simple image attributes such as luminance and contrast information (2) to Gestalt rules of perceptual organization such as proximity and good continuation (3, 4), known properties of perceptual systems appear tuned to the statistics of natural images (5–8). As a whole, these studies support the hypothesis that human visual processing has evolved to efficiently encode images from our natural environment (see ref. 1 for a recent review). Here, we directly address this hypothesis by asking if, when the visual system must choose between two competing inputs, it prefers the one most representative of the natural environment.

During binocular rivalry, conscious perception alternates between different images presented to the two eyes. It is well established that some stimuli are preferred to others, for example, high-contrast stimuli will dominate over low-contrast stimuli, and thus will be perceived for a greater proportion of the presentation time (9, 10). Because most basic research into rivalry has used simple line or grating stimuli (the properties of which can be easily manipulated), relatively little is known about how the properties of broadband stimuli, such as natural images, affect predominance during rivalry. Here, we consider aspects of the spatiotemporal structure of natural images (and image sequences) to which the visual system is known to be sensitive, the amplitude and phase spectra, and their influence on binocular rivalry competition.

Amplitude Spectrum. The amplitude spectrum describes the distribution of energy across different spatiotemporal scales in an image. It is generally held that, for natural scenes, amplitude reduces with spatial and temporal frequency, such that $A(f) \propto 1/f^{\alpha}$, where A is amplitude, f is frequency, and α typically takes on values close to unity (6, 11–13), at least when averaging over an ensemble of images (14).

As evidenced earlier, the statistical utility of a variety of perceptual cues has been established for natural images, and it follows that human vision is also optimized (see ref. 7) to process stimuli with a $1/f$ amplitude spectrum. One instance of this is that the variances across a population of model neurons (with octave bandwidths) are equal when α is equal to 1 (6). Neurons in early visual cortex (i.e., V1) process images by band-pass filtering, so their analysis of visual information can be considered to be optimally efficient (15, 16). Furthermore, it has been demonstrated that the correlational structure of adult human contrast sensitivity data displays a power law consistent with natural images (13, 17).

Behaviorally, discrimination of changes in amplitude spectrum is most accurate when α is approximately 1.5 spatially (18–21) and α is between 0.8 and 1 temporally (21). Surround suppression is stronger with surrounds of natural amplitude spectra compared with less natural surrounds (22). Moreover, visual noise is most effective at evoking mental imagery (23) and inducing visual hallucinations (24) when it has a fractal dimension consistent with natural images. Studies of visual art have also been shown to display a similar fractal structure (25, 26).

We hypothesize that this preference for images with natural amplitude spectra might also be reflected by the rivalry process, with the dominant stimulus in a pair being that for which α is closest to unity. As the amplitude spectra for natural images are similar in the spatial and temporal domains (12), we should expect similar results for (*i*) varying the spatial amplitude spectrum of static noise images, and (*ii*) varying the temporal amplitude spectrum of a dynamic noise sequence.

Phase Spectrum. Whereas the amplitude spectrum determines the amount of energy at each spatial (or temporal) scale, the phase spectrum specifies how the energy is distributed across the image. Natural images contain congruencies in the phase spectrum across spatial scales, which correspond to edges and features in a visual scene, and are critical in determining image content and appearance (27–30). Scrambling (i.e., randomizing) the phase spectrum produces an image with an identical amplitude spectrum, but without recognizable structure.

Although phase-scrambled images are frequently used as control stimuli, particularly in neuroimaging studies (31–33), they have rarely been used in psychophysical studies of binocular rivalry. One exception is a recent study by Alais and Melcher

Author contributions: D.H.B. and E.W.G. designed research; D.H.B. and E.W.G. performed research; D.H.B. analyzed data; and D.H.B. and E.W.G. wrote the paper.

The authors declare no conflict of interest.

This article is a PNAS Direct Submission.

[1]To whom correspondence should be addressed. E-mail: d.h.baker@soton.ac.uk.

 www.pnas.org/cgi/doi/10.1073/pnas.0812860106

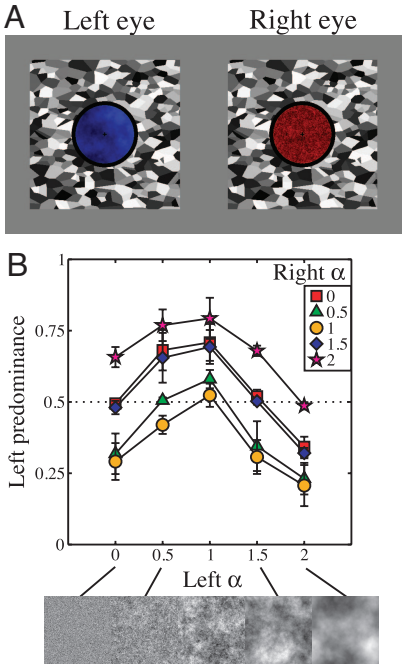

Fig. 1. Example stimuli and results of experiment I. (*A*) Example static noise stimuli shown to left and right eyes, tinted blue and red to aid identification. The surrounding binocular ring and Voronoi texture aided fusion. (*B*) Results averaged across 4 observers and expressed as left predominance—the proportion of time the left image was reported as seen—as a function of α for the left eye. The terms ''left'' and ''right'' are used for convenience only, as in the experiment these were counterbalanced. Note that data points where both images had the same exponent sit near the horizontal dotted midline, indicating that they were equally dominant.

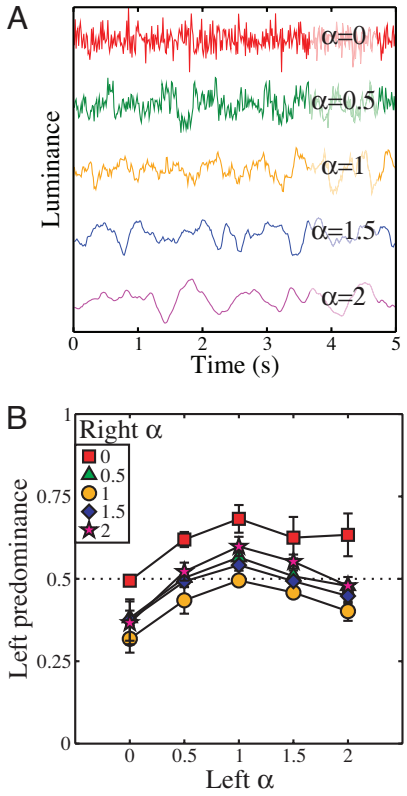

Fig. 2. Temporal luminance profiles and results of experiment II. (*A*) Example luminance profiles of a single pixel at different temporal α values. The functions are displaced vertically for clarity. (*B*) Results for experiment II, displayed in the same format as those in Fig. 1*B*. Here, α gives the exponent determining the temporal amplitude spectrum.

(34), in which images of faces and houses are rivaled with each other or with their phase-scrambled counterparts. Suppression was shown to be more coherent (i.e., less piecemeal rivalry reported) between 2 images with intact phase spectra than when one image was phase-randomized. However, we are aware of no reports of the effect of phase scrambling on image dominance during rivalry.

Present Study. Three experiments were devised to explore these issues. In the first 2, noise images with different spectral properties in either the spatial (i.e., experiment I) or temporal (i.e., experiment II) domain engaged in binocular rivalry. As predicted, the greatest dominance was found for images where α is equal to 1. The third experiment revealed that images with natural phase spectra dominate strongly over their phase-scrambled counterparts. These findings indicate that the binocular rivalry process favors stimuli with natural properties, consistent with the notion that the visual system is optimized for the encoding of the spatiotemporal structure of natural images (1).

Experiment I: Static Noise Images. We began by measuring dominance during binocular rivalry between static filtered noise images with different spectral slopes. Five values of α were used, with factorial combination resulting in 15 unique pairings. The images were tinted red or blue (Fig. 1*A*), and observers responded to the color of an image they perceived throughout each trial (35).

Experiment I Results. Fig. 1*B* shows predominance data averaged across all 4 subjects. For all functions, predominance peaks when α equals 1. This indicates that images with natural amplitude spectra will tend to dominate in binocular rivalry against images with both larger and smaller α values. There is a distinct asymmetry to the functions, with the falloff in predominance toward lower α values being approximately half as steep as at higher α values. This pattern of results was seen for all observers.

Experiment II: Dynamic Noise Sequences. The second experiment used the same design, but this time the rivalry stimuli consisted of temporally filtered dynamic noise sequences (e.g., refs. 21, 36). The amplitude spectrum exponent was fixed at an α value of 1 in the spatial domain, but varied in the temporal domain as the independent variable. Plots of luminance variation over time for single pixels at each temporal exponent value are illustrated in Fig. 2*A*.

Experiment II Results. Fig. 2*B* shows the results, averaged over 4 observers. These are qualitatively similar to the spatial data of experiment I, also showing a peak at an α value of 1, which was again consistent across all observers. The magnitude of modulation is slightly smaller than in the spatial domain, and less asymmetry is apparent—here the smaller α values are weakest. Nevertheless, there is clear evidence that the rivalry system favors dynamic image sequences with natural properties.

Analysis. Behaviorally, a peak at an α value of 1 is consistent with several previous studies (using unambiguous stimuli), which have explored discrimination performance (18, 19) and perceived contrast (22) for static filtered noise images. As binocular rivalry is particularly dependent on stimulus contrast, we kept the root

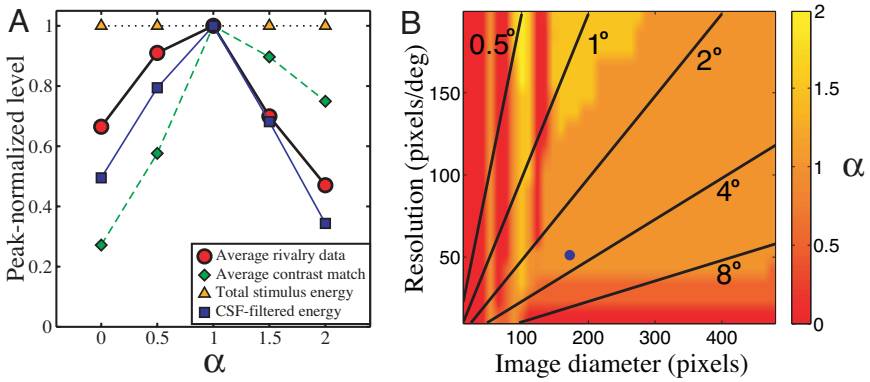

Fig. 3. Analysis of scaling metrics for fractal noise stimuli. (*A*) Peak-normalized functions for (*i*) rivalry data from Fig. 1*B* averaged across condition (red circles), (*ii*) contrast matching data, averaged over 3 observers (green diamonds), (*iii*) total stimulus energy (orange triangles), and (*iv*) effective contrast of noise stimuli after attenuation by a model CSF (blue squares). (*B*) Intensity map showing the strongest α value averaged over 100 simulations of the effective contrast model (note that the peak varied across successive simulations in only a small number of cases). The blue circle corresponds to the stimulus dimensions from experiment I, and radial lines indicate stimulus size in degrees of visual angle.

mean square (RMS) contrast of our noise images constant throughout (37). This means that the total stimulus energy was identical for all values of α (orange triangles in Fig. 3*A*). However, we wondered if the effective contrast of the noise was also constant, in terms of (*i*) perceived contrast or as (*ii*) suprathreshold contrast energy, following attenuation by the contrast sensitivity function (CSF). [Note that these are not equivalent as a result of the contrast constancy effect (38), whereby appearance is veridical for high-contrast stimuli despite differences in sensitivity.] We explored the first possibility behaviorally by using contrast matching and the second computationally by combining amplitude spectra with a model CSF.

The contrast matching task was completed by 3 observers who participated in experiment I, and is described in the *Materials and Methods* section. The results in Fig. 3*A* (green diamonds) indicate the perceived contrast of each (static) $1/f^{\alpha}$ noise stimulus, as matched to a standard grating stimulus of 3 c/°. Data were averaged across observers and peak-normalized. Shown for comparison are the rivalry data of experiment I, also peak-normalized and averaged across all 5 functions (red circles). Although both functions do peak at an α of 1, it is clear that the falloff in perceived contrast does not mirror the rivalry dominance data. Perceived contrast is greater at larger α values, and much lower at smaller α values, relative to the rivalry results. It therefore seems unlikely that perceived contrast is responsible for our findings.

For the computational analysis, we estimated a typical CSF by fitting a second-order polynomial to a public contrast sensitivity data set [ModelFest (39)]. We then multiplied points on this model CSF by each bin of the amplitude spectra of the filtered noise images, and pooled across bins to give an estimate of the suprathreshold contrast "energy" (e.g., ref. 40) for each image type. These values were peak-normalized, and are shown in Fig. 3*A* (blue squares) along with the rivalry and matching data. As well as peaking at an α of 1, the suprathreshold contrast estimates were much closer to the rivalry data than were the contrast matches. This is impressive, particularly as the effective contrast model did not incorporate individual differences in sensitivity, which would be expected to influence the pattern of results somewhat.

To confirm that this finding was not peculiar to our stimulus configuration, we repeated the analysis over a wide range of image diameters (12–480 pixels) and resolutions (10–200 pixels/°), finding the peak of the resulting function to be at an α of 1 for many combinations (61%; see Fig. 3*B*). Only when images had few pixels (<100), low resolution (<40 pixels/°), or limited extent (<1.5°) did the peak of the function differ from an α of 1. We found a similar pattern (not shown) when pixel luminance was scaled to cover the available dynamic range (e.g., ref. 22), rather than having a fixed RMS contrast as in our experiments.

The conditions yielding effective contrast functions that peak at an α of 1 suggest that, across the range of images likely to be encountered by the visual system in the natural world, or indeed in laboratory experiments, effective contrast is (on average) maximal for images with a natural amplitude spectrum (for a related approach, see refs. 13, 17). Given the strong contrast dependency of binocular rivalry (9, 10), more naturalistic images (which are most likely to contain behaviorally relevant information) will typically dominate over less natural ones. Furthermore, our analysis indicates that the crucial factor for binocular rivalry is neither perceived nor physical (i.e., RMS or Michelson) contrast. Instead, we find that effective contrast (i.e., the total energy at each frequency, relative to detection threshold) offers a better explanation. By extension, we assume that similar constraints apply to the temporal data of experiment II.

Experiment III: Natural and Phase-Scrambled Images. In this experiment, natural images engaged in rivalry with their phase-scrambled counterparts. This ensured that the amplitude spectrum for each image pair was identical, so any variation in dominance can be attributed to the differences in phase information. We were concerned that recognizable features in natural images might bias observers to report them as dominant. To assess this, we included a rivalry simulation condition, detailed later, in which regions of a binocularly presented stimulus alternated between the natural and phase-scrambled image (41).

Experiment III Results. The results of experiment III are shown in Fig. 4*A* and are very clear. The red bars give the predominance of 8 natural images over their phase-scrambled counterparts. The natural image was dominant more than 50% of the time for all images and for all observers, with a mean predominance of 69.5%. ANOVA revealed a highly significant effect of image phase ($F = 329.57$, $p \ll 0.001$; all individual subject ANOVAs were also significant).

In the simulation condition (yellow bars), natural images were dominant for 51.4% of the total presentation (mean). This is close to the proportion of each image type actually displayed during simulations (50%), and an ANOVA found no effect of image phase ($F = 0.72$, $p > 0.41$). We used the simulation data

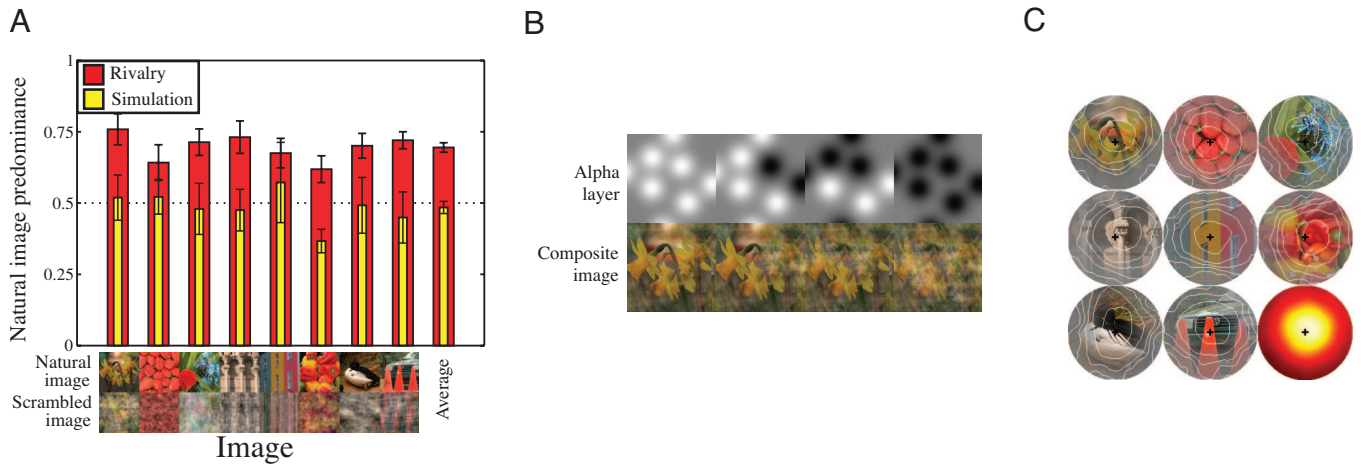

Fig. 4. Results and example stimuli for experiment III, in which natural images rivaled with their phase-scrambled counterparts. (*A*) Data plotted as the proportion of time the natural image was reported as dominant during rivalry (red) and simulation (yellow) conditions, for 8 images. The average across all images is given by the bar (*Right*). Data are averaged across 6 observers, with error bars showing ± 1SE. In the rivalry conditions, the natural images were seen for the majority of each trial. (*B*) Example stimuli from the replay condition—the alpha layer (*Upper*) determines transparency of the natural image. As the Gaussians comprising the alpha layer were varied over time, they produced a range of composite images, as shown (*Lower*). (*C*) Correlation maps show how the state of each pixel (natural or scrambled image) is predictive of observer responses (average of 6 observers). The contrast of each pixel is scaled in proportion to its correlation coefficient (*r*), and contours enclose the 10th-, 30th-, 50th-, 70th-, and 90th-percentile *r* values. The lower right circle is an intensity map of *r* averaged across all 8 images.

to determine whether some image regions were more predictive of observer responses than others, which would indicate a reporting bias for specific, recognized features of the phase-intact images. We first assessed observer response latencies by finding the peak in the cross-correlation function between the response time course and the proportion of the stimulus in the natural versus the phase-scrambled state. The mean latency across observers was 895 ± 102 ms. We then calculated the correlation between observer responses and the image state of each pixel over our presentation sequences at the appropriate latency for each observer. Averaged over multiple trials (and observers), this allowed us to generate a "map" of the areas of the image that were most predictive of behavioral responses, as shown in Fig. 4*C*. These maps all peaked around the fixation point, with no obvious areas of inhomogeneity corresponding to specific image features (e.g., objects, surfaces, or edges). Thus, our observers showed no consistent bias relating to image features during a rivalry-like task, and were unlikely to have exhibited such biases during the regular binocular rivalry trials.

Discussion

Three experiments demonstrated the preference of the binocular rivalry system for stimulus properties associated with natural images. In both the spatial and temporal domain, noise images with an amplitude spectrum of $1/f$ dominated over all other spectral slopes tested. When the amplitude spectrum was fixed, images with natural phase spectra dominated over those with randomized phase spectra. These findings suggest that the mechanisms of binocular rivalry, in common with other aspects of the visual system, are preferentially selective for natural images.

Temporal Aspects of Rivalry. Despite a plethora of studies on the spatial aspects of rivalry, its temporal behavior been explored less extensively. When stimuli are defined by spatial form but also have a temporal component, rivalry is usually possible provided the temporal frequencies are similar (42, 43). Over a limited range, faster stimuli will dominate over slow or static stimuli (44–47). However, this is by no means a general property; for some dichoptic motion combinations, faster stimuli are less dominant (46). Furthermore, for stimuli differing greatly in temporal content (43) or defined only by temporal frequency [i.e., a flickering field containing no form information (42)] a fused or transparent percept is seen instead of rivalry. Based on this evidence, it has been proposed that two distinct motion channels undergo independent rivalry and do not interact with each other (43).

The dynamic noise samples used in experiment II contained energy at a wide range of temporal frequencies (1–37 Hz, or a range of >5 octaves). Perhaps because of their broadband nature, normal rivalry alternations occurred in all cases, with observers easily able to report the colored tint of the dominant stimulus. For extreme motion differences ($\alpha = 0$ vs. $\alpha = 2$) there was some awareness of faster motion when perceiving the slower stimulus. This is probably related to dichoptic motion transparency (43), although we stress that the form and color information always rivaled normally [i.e., there was no evidence of "misbinding" (48), which occurs under certain circumstances]. It was also not the case that faster stimuli (i.e., those with the most high temporal frequency energy, at $\alpha = 0$) were more dominant; in fact, they were weakest (Fig. 2*B*). Instead, the rivalry process favored stimuli with a balance of low and high frequencies corresponding to that observed in the natural environment.

Implications of Phase Scrambling. What image properties might produce the result that images with natural phase spectra dominate over their phase-scrambled counterparts? Mante et al. (2) have shown that luminance and contrast are correlated in phase-scrambled images, but are statistically independent in natural images (although see also ref. 49). This de-correlation is reflected in the early visual system, which has independent gain control processes for luminance and contrast. As both of these dimensions are important attributes for rivalry (9), it is possible that stimuli conforming to this de-correlation (i.e., natural images) are favored by the sparse coding strategy of the visual system (50). In addition, phase-scrambling an image also removes the phase congruencies across spatial scales that are characteristic of image features (28). Complex cells in V1 are selective for such image features, and so produce greater re-

sponses to natural images (51), which might equate to stronger input at early stages of the rivalry hierarchy.

Alternatively, recent functional MRI evidence (52) has demonstrated that, whereas V1 responds largely to contrast energy, extra-striate areas are strongly driven by stimuli containing contours. This activation might influence rivalry in higher brain areas, or modulate earlier activity via feedback connections. Indeed, it has recently been demonstrated (53) that the presence of continuous contours [which are statistically frequent in natural images (8)] can bind together alternations during rivalry, increasing synchronization between individual image regions. This provides a plausible mechanism by which images with natural phase spectra might both obtain greater dominance and produce more coherent alternations (34).

Rivalry Within a Larger Scene. Other image properties can play a major role in binocular rivalry. Contextual information in many domains, including color (54, 55), global motion (56), surround orientation (55, 57, 58), surround motion (47, 59), percept history (60), and depth information (61), can also influence the pattern of dominance during rivalry in a variety of ways. Furthermore, it has been demonstrated that coherent visual objects, such as houses or faces, produce deeper rivalry suppression with more global (and fewer piecemeal) alternations, compared with simple grating stimuli (34). These findings indicate that contextually rich stimuli, which incorporate aspects beyond the low-level features of the rivaling stimulus, are important in determining rivalry behavior.

Conclusions

Surprisingly, previous studies of binocular rivalry have not explicitly explored the role of natural image statistics, despite the general success of this approach in explaining other aspects of visual performance (1, 2, 5–8, 11, 18, 19, 22, 27–29). Here, we have demonstrated that natural images are strongly preferred by the rivalry system in both the spatial and temporal domain. We propose that the high effective contrast of natural images, and phase congruencies corresponding to contours, may be responsible for this preference.

Materials and Methods

Apparatus and Stimuli. All stimuli were presented on a ViewSonic G90fB monitor (mean luminance 60 cd/m^2, γ-corrected), running at 75 Hz, using a GeForce 7300GT high performance graphics card (NVIDIA) and an Apple Macintosh computer. The Psychophysics Toolbox routines (62, 63), running under Matlab 7.4 (Mathworks), were used to display stimuli. Dichoptic presentation of images was achieved using a mirror stereoscope.

For experiment I, stimuli were static patches of Gaussian noise, generated on the fly for each trial, subtending 3.3° of visual angle (172 pixels). The noise was filtered in the Fourier domain so that it had an amplitude spectrum proportional to $1/f^{\alpha}$, where α took on values of 0, 0.5, 1, 1.5, and 2. At these dimensions and resolution, the stimuli contained spatial frequency components between 0.3 and 25 c/°. After filtering, the pixel values were scaled so that each noise patch had an RMS contrast of 0.3. Stimulus examples are shown in Fig. 1*A* and along the lower axis of Fig. 1*B*.

Experiment II used smaller noise stimuli, 1.5° in diameter, so that on-the-fly spatiotemporal filtering was achievable between trials. The spatial amplitude spectrum exponent was always at an α of 1, while the exponent in the temporal domain took on values between 0 and 2. A 5-second movie sequence was generated for each stimulus, and this was looped for the trial duration (note that, because of the periodic nature of the Fourier transform, there was no temporal discontinuity when looping the stimuli). Stimuli contained temporal components between a 1-Hz lower limit and the Nyquist limit of 37 Hz, determined by the monitor refresh rate. The lower limit was imposed to ensure that stimuli were not constructed with the majority of their energy at very low temporal frequencies, making them appear static.

All noise stimuli were tinted red or blue by using only one gun of the CRT for each stimulus. In pilot experiments we determined the relative predominance of patches of red and blue luminance for each observer. For most observers these were approximately equal when each gun used its full luminance range. One observer (E.W.G.) showed a strong bias for red, which was compensated for by attenuating the output of the red channel by a factor of 2 using lookup tables. Lookup table scaling ensured that the contrast resolution of the stimuli was identical for all observers.

Stimuli for experiment III were 8 images selected from the McGill calibrated color image database (http://tabby.vision.mcgill.ca), shown along the lower axis of Fig. 4*A*. The selected images contained a range of natural and man-made objects, and a region subtending 3° (154 pixels) was extracted for use in the experiment. Each image was Fourier transformed, and the phase spectrum replaced by a random-phase spectrum (obtained from Gaussian noise) before applying an inverse Fourier transformation. The random-phase spectrum was identical for each color layer (i.e., red/green/blue) in the image, so the phase-scrambled versions retained the same palette as the original images. A new phase-scrambled image was generated for each trial. We ensured that RMS contrast was equal for each image pair by scaling the contrast of the original image as required.

Procedure. Observers were seated in a darkened room and viewed the monitor through the stereoscope at a total viewing distance of 85.5 cm. They indicated their percept (red or blue image for experiments I and II, natural or phase-scrambled image for experiment III) continuously using the keyboard. As piecemeal rivalry sometimes occurs for extended images, they were instructed to base their responses on the dominant image, i.e., that which covered the majority of the aperture. To aid fusion during presentation, each stimulus patch was surrounded by a dark ring (0.1° thick). Outside the ring, a large Voronoi texture (see Fig. 1*A*) was displayed to both eyes. Finally, a small dark fixation cross was present in the center of each stimulus.

Stimuli were presented in 1-minute trials, and were always counterbalanced across eye of presentation and (in experiments I and II) red/blue tinting. Each condition was repeated 20 (experiments I and II) or 12 (experiment III) times by each observer. Data were pooled across repetition, eye of presentation, and color allocation (experiments I and II). The predominance of each image in a pair was calculated as the proportion of responses indicating that image was seen (i.e., discounting times at which no key was pressed). The results were very similar for all observers, with all variations being of magnitude rather than of kind. For this reason, we averaged across observers to present the results.

In experiment III, an equal number of simulation trials, in which a ''movie'' of composite images was presented binocularly, were interleaved with the rivalry trials. The purpose of these simulation trials was to establish whether observers had a bias to report the phase-intact images over the phase-scrambled images. To generate these, we extended the procedure of Lee and Blake (41). Eight image locations were randomly determined, separated by at least 1°, each of which defined the centre of a 2D Gaussian function ($\sigma = 0.3°$). Over time, the polarity of each Gaussian function was varied according to durations drawn from a γ-distribution (mean duration, 2.5 s), with the final time course smoothed by convolution to produce smooth transitions. The 8 Gaussians were applied to the alpha (i.e., transparency) channel of the natural (i.e., red/green/blue/alpha) image, causing some regions to be transparent, and revealing the scrambled image. Example composite images created in this way are shown in Fig. 4*B*. In the left-most image, all Gaussians are positive, and show mostly the natural image (gray regions in the α-layer correspond to a 50/50 mix of the 2 images), whereas in the right-most image, all Gaussians are negative, revealing mostly the phase-scrambled image. This procedure produced a similar effect to piecemeal rivalry, forcing observers to base their responses on a judgment of which image was most dominant. Any bias should therefore show up much more readily using this paradigm than using a standard replay procedure in which the entire image was in one or the other state.

Contrast Matching. Observers matched the contrast of the noise patches used in experiment I to a horizontal grating of spatial frequency 3 c/°, which varied in contrast. All stimuli were 5° in diameter, spatially limited by a raised cosine function, and presented for 200 ms. Stimuli were presented centrally outside of the stereoscope and were luminance-defined (i.e., grayscale; color tinting was not used). A 2IFC procedure (i.e., 1-up, 1-down ''staircase'') was used to measure the point of subjective equality, which was estimated from the psychometric function using Probit analysis (64).

Observers. Both authors and 2 naïve observers participated in experiments I and II (one naïve observer participated in both, whereas the other differed across experiments). Experiment III was completed by the first author and 5 naïve observers. All observers were psychophysically experienced and wore their normal optical correction during testing. Experiments were approved by the local ethics committee and adhered to the principles of the Declaration of Helsinki, and informed consent was obtained from all observers.

ACKNOWLEDGMENTS. This work was supported by Biotechnology and Biological Sciences Research Council grant BB/E012698/1.

1. Geisler WS (2008) Visual perception and the statistical properties of natural scenes. *Annu Rev Psychol* 59:167–192.
2. Mante V, Frazor RA, Bonin V, Geisler WS, Carandini M (2005) Independence of luminance and contrast in natural scenes and in the early visual system. *Nat Neurosci* 8:1690–1697.
3. Brunswick E, Kamiya J (1953) Ecological cue validity of 'proximity' an other Gestalt factors. *Am J Psych* 66:20–32.
4. Elder JH, Goldberg RM (2002) Ecological statistics of Gestalt laws for the perceptual organisation of contours. *J Vis* 2:324–353.
5. Maloney LT (1986) Evaluation of linear models of surface spectral reflectance with small numbers of parameters. *J Opt Soc Am A* 3:1673–1683.
6. Field DJ (1987) Relations between the statistics of natural images and the response properties of cortical cells. *J Opt Soc Am A* 4:2379–2394.
7. Simoncelli EP, Olshausen BA (2001) Natural image statistics and neural representation. *Annu Rev Neurosci* 24:1193–1216.
8. Geisler WS, Perry JS, Super BJ, Gallogly DP (2001) Edge co-occurrence in natural images predicts contour grouping performance. *Vision Res* 41:711–724.
9. Levelt WJM (1966) The Alternation Process In Binocular Rivalry. *Br J Psychol* 57:225–238.
10. Mamassian P, Goutcher R (2005) Temporal dynamics in bistable perception. *J Vis* 5:361–375.
11. Burton GJ, Moorhead IR (1987) Color and spatial structure in natural scenes. *Appl Optics* 26:157–170.
12. Dong DW, Atick JJ (1995) Statistics of natural time-varying images. *Network Comput Neural Syst* 6:345–358.
13. Billock VA, de Guzman GC, Kelso JAS (2001) Fractal time and 1/f spectra in dynamic images and human vision. *Physica D* 148:136–146.
14. Langer MS (2000) Large-scale failures of f^{α} scaling in natural image spectra. *J Opt Soc Am A Opt Image Sci Vis* 17:28–33.
15. Attneave F (1954) Some informational aspects of visual perception. *Psychol Rev* 51:183–193.
16. Barlow HB (1961) Possible principles underlying the transformations of sensory messages. S*ensory communication*, ed Rosenblith WA (MIT Press, Cambridge, MA), pp 217–234.
17. Billock VA (2000) Neural acclimation to 1/f spatial frequency spectra in natural images transduced by the human visual system. *Physica D* 137:379–391.
18. Tadmor Y, Tolhurst DJ (1994) Discrimination of changes in the second-order statistics of natural and synthetic images. *Vision Res* 34:541–554.
19. Knill DC, Field D, Kersten D (1990) Human discrimination of fractal images. *J Opt Soc Am A* 7:1113–1123.
20. Hansen BC, Hess RF (2006) Discrimination of amplitude spectrum slope in the fovea and parafovea and the local amplitude distributions of natural scene imagery. *J Vis* 6:696–711.
21. Billock VA, Cunningham DW, Havig PR, Tsou BH (2001) Perception of spatiotemporal random fractals: an extension of colorimetric methods to the study of dynamic texture. *J Opt Soc Am A Opt Image Sci Vis* 18:2404–2413.
22. McDonald JS, Tadmor Y (2006) The perceived contrast of texture patches embedded in natural images. *Vision Res* 46:3098–3104.
23. Rogowitz BE, Voss RF (1990) Shape perception and low-dimension fractal boundary contours. *Proc SPIE* 1249:387–394.
24. Billock VA, Tsou BH (2007) Neural interactions between flicker-induced self-organized visual hallucinations and physical stimuli. *Proc Natl Acad Sci USA* 104:8490–8495.
25. Redies C, Hasenstein J, Denzler J (2007) Fractal-like image statistics in visual art: similarity to natural scenes. *Spat Vis* 21:137–148.
26. Taylor RP, Micolich AP, Jonas D (1999) Fractal analysis of Pollock's drip paintings. *Nature* 399:422.
27. Hansen BC, Hess RF (2007) Structural sparseness and spatial phase alignment in natural scenes. *J Opt Soc Am A Opt Image Sci Vis* 24:1873–1885.
28. Kovesi P (2000) Phase congruency: a low-level image invariant. *Psychol Res* 64:136–148.
29. Tadmor Y, Tolhurst DJ (1993) Both the phase and the amplitude spectrum may determine the appearance of natural images. *Vision Res* 33:141–145.
30. Oppenheim AV, Lim JS (1981) The importance of phase in signals. *Proc IEEE* 69:529–541.
31. Tsao DY, Freiwald WA, Knutsen TA, Mandeville JB, Tootell RB (2003) Faces and objects in macaque cerebral cortex. *Nat Neurosci* 6:989–995.
32. Simmons WK, Martin A, Barsalou LW (2005) Pictures of appetizing foods activate gustatory cortices for taste and reward. *Cereb Cortex* 15:1602–1608.
33. Xu Y, Turk-Browne NB, Chun MM (2007) Dissociating task performance from fMRI repetition attenuation in ventral visual cortex. *J Neurosci* 27:5981–5985.
34. Alais D, Melcher D (2007) Strength and coherence of binocular rivalry depends on shared stimulus complexity. *Vision Res* 47:269–279.
35. Moutoussis K, Keliris G, Kourtzi Z, Logothetis N (2005) A binocular rivalry study of motion perception in the human brain. *Vision Res* 45:2231–2243.
36. Cass J, Alais D (2006) Evidence for two interacting temporal channels in human visual processing. *Vision Res* 46:2859–2868.
37. Moulden B, Kingdom F, Gatley LF (1990) The standard deviation of luminance as a metric for contrast in random-dot images. *Perception* 19:79–101.
38. Georgeson MA, Sullivan GD (1975) Contrast constancy: deblurring in human vision by spatial frequency channels. *J Physiol* 252:627–656.
39. Watson AB, Ahumada AJJ (2005) A standard model for foveal detection of spatial contrast. *J Vis* 5:717–740.
40. Tolhurst DJ, Tadmor Y (1997) Band-limited contrast in natural images explains the detectability of changes in the amplitude spectra. *Vision Res* 37:3203–3215.
41. Lee S-H, Blake R (2004) A fresh look at interocular grouping during binocular rivalry. *Vision Res* 44:983–991.
42. O'Shea RP, Blake R (1986) Dichoptic temporal frequency differences do not lead to binocular rivalry. *Percept Psychophys* 39:59–63.
43. van de Grind WA, van Hof P, van der Smagt MJ, Verstraten FA (2001) Slow and fast visual motion channels have independent binocular-rivalry stages. *Proc Biol Sci* 268:437–443.
44. Wade NJ, de Weert CM, Swanston MT (1984) Binocular rivalry with moving patterns. *Percept Psychophys* 35:111–122.
45. Wiesenfelder H, Blake R (1990) The neural site of binocular rivalry relative to the analysis of motion in the human visual system. *J Neurosci* 10:3880–3888.
46. Blake R, Yu K, Lokey M, Norman H (1998) Binocular rivalry and motion perception. *J Cogn Neurosci* 10:46–60.
47. Baker DH, Graf EW (2008) Equivalence of physical and perceived speed in binocular rivalry. *J Vis* 8(4):26, 1–12.
48. Hong SW, Shevell SK (2006) Resolution of binocular rivalry: perceptual misbinding of color. *Vis Neurosci* 23:561–566.
49. Lindgren JT, Hurri J, Hyvarinen A (2008) Spatial dependencies between local luminance and contrast in natural images. *J Vis* 8(12):6, 1–13.
50. Olshausen BA, Field DJ (1996) Emergence of simple-cell receptive field properties by learning a sparse code for natural images. *Nature* 381:607–609.
51. Felsen G, Touryan J, Han F, Dan Y (2005) Cortical sensitivity to visual features of natural scenes. *PLoS Biol* 3:e342.
52. Dumoulin SO, Dakin SC, Hess RF (2008) Sparsely distributed contours dominate extra-striate responses to complex scenes. *Neuroimage* 42:890–901.
53. Alais D, Lorenceau J, Arrighi R, Cass J (2006) Contour interactions between pairs of Gabors engaged in binocular rivalry reveal a map of the association field. *Vision Res* 46:1473–1487.
54. Kovacs I, Papathomas TV, Yang M, Feher A (1996) When the brain changes its mind: interocular grouping during binocular rivalry. *Proc Natl Acad Sci USA* 93:15508–15511.
55. Paffen CLE, Tadin D, te Pas SF, Blake R, Verstraten FAJ (2006) Adaptive center-surround interactions in human vision revealed during binocular rivalry. *Vision Res* 46:599–604.
56. Alais D, Blake R (1998) Interactions between global motion and local binocular rivalry. *Vision Res* 38:637–644.
57. Fukuda H, Blake R (1992) Spatial interactions in binocular rivalry. *J Exp Psychol Hum Percept Perform* 18:362–370.
58. Ichihara S, Goryo K (1978) The effects of relative orientation of surrounding gratings on binocular rivalry and apparent brightness of central gratings. *Jpn Psych Res* 20:159–166.
59. Paffen CLE, te Pas SF, Kanai R, van der Smagt MJ, Verstraten FAJ (2004) Center-surround interactions in visual motion processing during binocular rivalry. *Vision Res* 44:1635–1639.
60. Brascamp JW, et al. (2008) Multi-timescale perceptual history resolves visual ambiguity. *PLoS ONE* 3:e1497.
61. Graf EW, Adams WJ (2008) Surface organization influences bistable vision. *J Exp Psychol Hum Percept Perform* 34:502–508.
62. Brainard DH (1997) The psychophysics toolbox. *Spat Vis* 10:433–436.
63. Pelli DG (1997) The VideoToolbox software for visual psychophysics: transforming numbers into movies. *Spat Vis* 10:437–442.
64. Finney DJ (1971) *Probit Analysis* (Cambridge Univ Press, Cambridge, UK).